

Supporting Information

Zocher et al. 10.1073/pnas.1210373109

SI Text

Unfolding β_2 -Adrenergic Receptor from N- and C-Terminal Ends. β_2 -Adrenergic receptor (β_2 AR) can attach nonspecifically with either the N- or C-terminal end to the atomic force microscopy (AFM) stylus. Accordingly, two different unfolding force–distance (F-D) spectra were recorded (Fig. S3). To assign these classes to N- or C-terminal unfolding, the N-terminal FLAG tag was enzymatically removed, and the shortened β_2 AR was unfolded (Fig. S4). A shift of ~ 14 aa was observed in one class of F-D curves, suggesting that this particular class corresponds to N-terminal unfolding. Approximately 70–80% of the F-D curves ($n \sim 1,000$) corresponded to the unfolding of β_2 AR by mechanically pulling the N-terminal end (Fig. S3A). The remaining

F-D curves represented unfolding of the receptor from the C-terminal end (Fig. S3B). The superimpositions of F-D curves showed a characteristic pattern of eight force peaks when unfolding β_2 AR from the N-terminal end (Fig. S3A). When unfolding β_2 AR from the C-terminal end, only four force peaks were detected (Fig. S3B). The C-terminal region of the receptor, which is unfolded at pulling distances < 30 nm, did not reveal reproducible unfolding events (force peaks) (Fig. S3B). In summary, F-D curves recording the unfolding of β_2 AR from the N-terminal end occurred at higher probability and most importantly, detected more unfolding events and interactions of the G protein-coupled receptor (GPCR). For these reasons, we analyzed only F-D curves that were recorded on unfolding of β_2 AR from the N-terminal end.

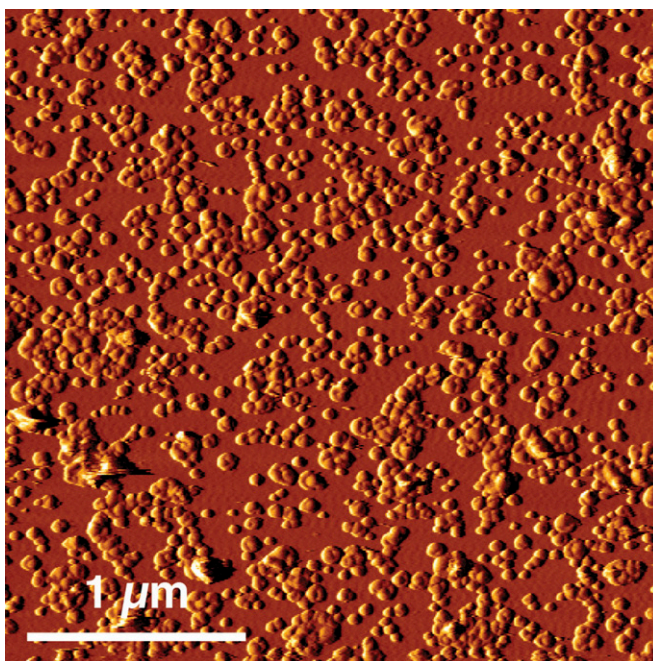


Fig. S1. AFM deflection image of β_2 AR proteoliposomes. Proteoliposomes were adsorbed overnight at 4 °C onto freshly cleaved mica in buffer solution (300 mM NaCl, 25 mM MgCl_2 , 25 mM Tris, pH 7.0). To remove weakly attached membrane patches, the sample was rinsed several times with the same buffer solution. Proteoliposomes protruded 7.7 ± 0.7 nm (average \pm SD, $n = 25$) from the mica surface. Native class A GPCRs have heights of ~ 7.8 nm (1). Thus, we conclude that, on adsorption to mica, the proteoliposomes opened and formed single-layered protein membranes. The diameter of these single-layered protein membranes ranged between 50 and 200 nm. The contact mode AFM deflection image was recorded in buffer solution applying an imaging force of ~ 50 –100 pN.

1. Fotiadis D, et al. (2003) Atomic-force microscopy: Rhodopsin dimers in native disc membranes. *Nature* 421(6919):127–128.

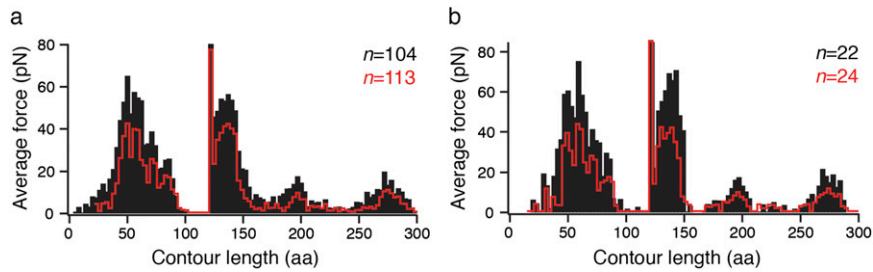


Fig. S2. Average force required to unfold structural segments of β_2 AR reconstituted into liposomes composed of phospholipids [1,2-dioleoyl-sn-glycero-3-phosphocholine (DOPC)] or phospholipids and cholesterol cholesteryl hemisuccinate (DOPC/CHS). (A) On average, the force required to unfold β_2 AR reconstituted into DOPC/CHS liposomes (black) was higher than the average force required to unfold β_2 AR reconstituted into DOPC liposomes (red). This difference implies an increased mechanical stability of the GPCR in the presence of cholesterol. To determine average unfolding forces, we calculated the sum of the unfolding force detected for every peak of every F-D curve superimposed in Fig. 1 B and C and divided this sum by the number of F-D curves analyzed. (B) To exclude that differences in average forces are not a result of cantilever calibration errors, β_2 AR in DOPC (red) and DOPC/CHS (black) liposomes was unfolded under identical experimental conditions using the same cantilever. F-D curves were aligned at the prominent force peak detected at a contour length of 121 aa. Bin sizes of histograms are 3 aa. The pulling velocity was 300 (A) and 528 nm/s (B); n indicates the numbers of F-D curves analyzed.

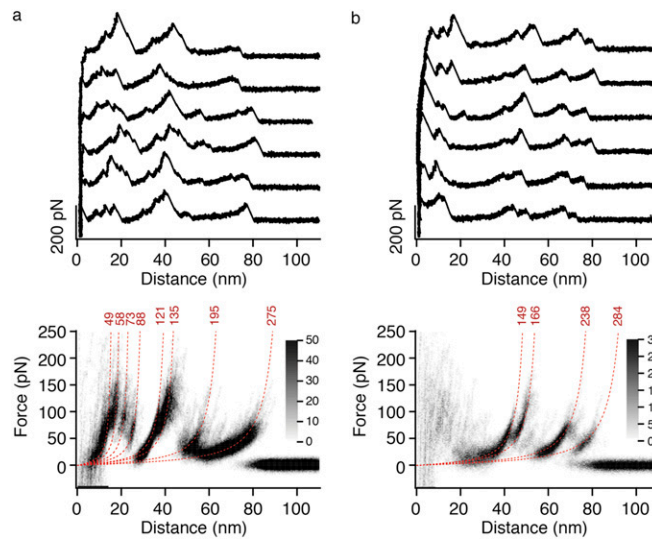


Fig. S3. N- and C-terminal unfolding of β_2 AR reconstituted into DOPC/CHS liposomes. Selection of F-D curves recorded on N- (A, Upper) and C-terminal (B, Upper) unfolding of β_2 AR. Superimpositions of F-D curves (density plots in A, Lower and B, Lower) highlight their common features. Red lines represent worm-like chain (WLC) curves fitting the force peaks. The number on top of each WLC curve indicates the average contour lengths (in amino acids) revealed from the fit. Gray scale bars allow evaluation of how frequently individual force peaks were populated. Single-molecule force spectroscopy (SMFS) data were recorded in SMFS buffer (300 mM NaCl, 25 mM Tris, 25 mM $MgCl_2$, pH 7.0). The number of superimposed F-D curves is $n = 103$ (A, Lower) and $n = 56$ (B, Lower).

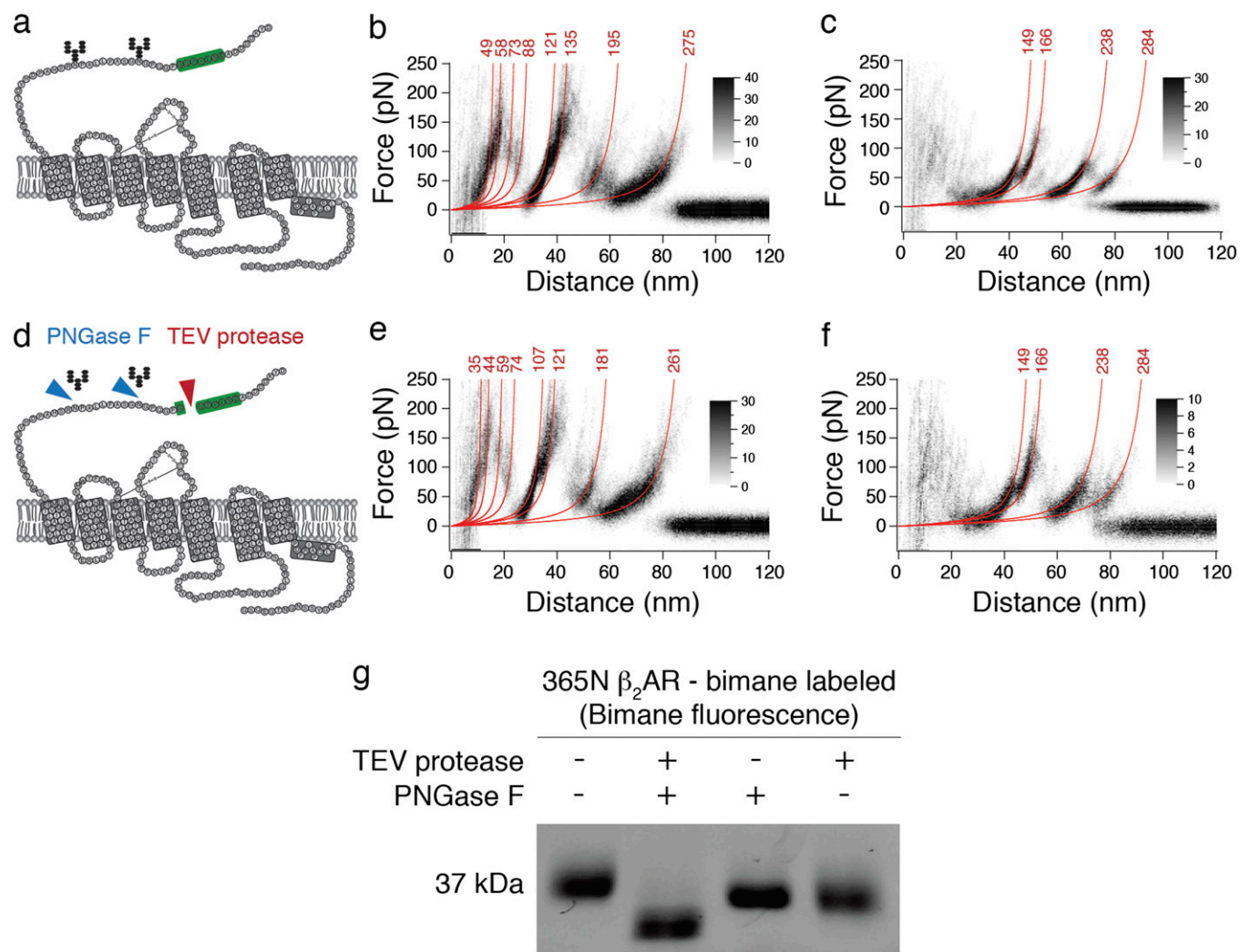


Fig. S4. Unfolding β_2 AR after removal of the FLAG tag. (A) Secondary structure model of 365N β_2 AR with N-terminal FLAG tag followed by a tobacco etch virus (TEV) protease cleavage site (colored in green). Superimposition of F-D curves recorded pulling the N- (B) and C-terminal (C) ends of β_2 AR before TEV protease treatment. SMFS of the untreated receptor shows the normal full-length spectrum. Force peaks were fitted using the WLC model to reveal the contour length of the unfolded and stretched polypeptide (given at the end of each WLC curve in amino acids). (D) Treatment of β_2 AR with TEV protease (red triangle) and PNGase F (blue triangles) removed 14 aa from the N terminus and removed the glycosylations, respectively. (E) Superimposition of F-D curves recorded on pulling the truncated N-terminal end of TEV protease-treated β_2 AR. On average, the force peaks showed a shift of 14 aa. (F) Superimposition of F-D curves recorded on pulling the C-terminal end of TEV protease-treated β_2 AR. All F-D curves were recorded in buffer solution (300 mM NaCl, 25 mM $MgCl_2$, 25 mM Tris, pH 7.0). The number of superimposed F-D curves was $n = 100$ (B), $n = 56$ (C), $n = 63$ (E), and $n = 20$ (F). (G) Bimane fluorescence stain of untreated, TEV protease-treated, and Peptide-N-Glycosidase F (PNGaseF) F-treated bimane-labeled β_2 AR. The molecular weight was shifted on the SDS gel after treatment with TEV, PNGaseF, and both enzymes.

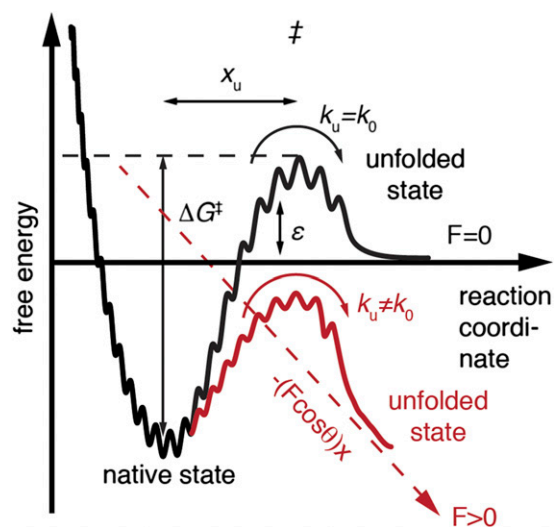


Fig. S5. Unfolding free-energy barrier-describing energetic (ΔG^\ddagger) and kinetic (k_0 and x_u) parameters of stable structural segments. According to the Bell–Evans theory (1, 2), folded structures can be characterized by a simple two-state model. A native folded structure resides in an energy valley and is separated by an energy barrier from the unfolded state. As approximated previously, the surface roughness of the free-energy landscape of transmembrane α -helices, ϵ , is $\sim 4\text{--}6 k_B T$ (3). This roughness generates local energy minima that can stabilize functionally related conformational states of a structural segment compared with a narrow energy valley. The transition state (\ddagger) has to be overcome to induce unfolding of the stable structural segment. x_u denotes the distance between the folded state and the transition state, k_0 represents the transition rate for crossing the energy barrier under zero force, and ΔG^\ddagger gives the activation energy for unfolding the stable structural segment. An externally applied force F changes the thermal likelihood of reaching the top of the energy barrier. The energy profile along the reaction coordinate (pulling direction) is tilted by the mechanical energy $-(F\cos\theta)x$, which is indicated by the red dashed line. The applied force does not change the distance between ground state and transition state x_u . θ defines the angle of the externally applied force relative to the reaction coordinate. As a result of this tilt, the energy barrier separating the folded state from the unfolded state decreases. Thus, the probability of the folded stable structural segment unfolding increases.

1. Evans E (1998) Energy landscapes of biomolecular adhesion and receptor anchoring at interfaces explored with dynamic force spectroscopy. *Faraday Discuss* 111(111):1–16.
2. Evans E (2001) Probing the relation between force—lifetime—and chemistry in single molecular bonds. *Annu Rev Biophys Biomol Struct* 30:105–128.
3. Janovjak H, Knaus H, Muller DJ (2007) Transmembrane helices have rough energy surfaces. *J Am Chem Soc* 129(2):246–247.

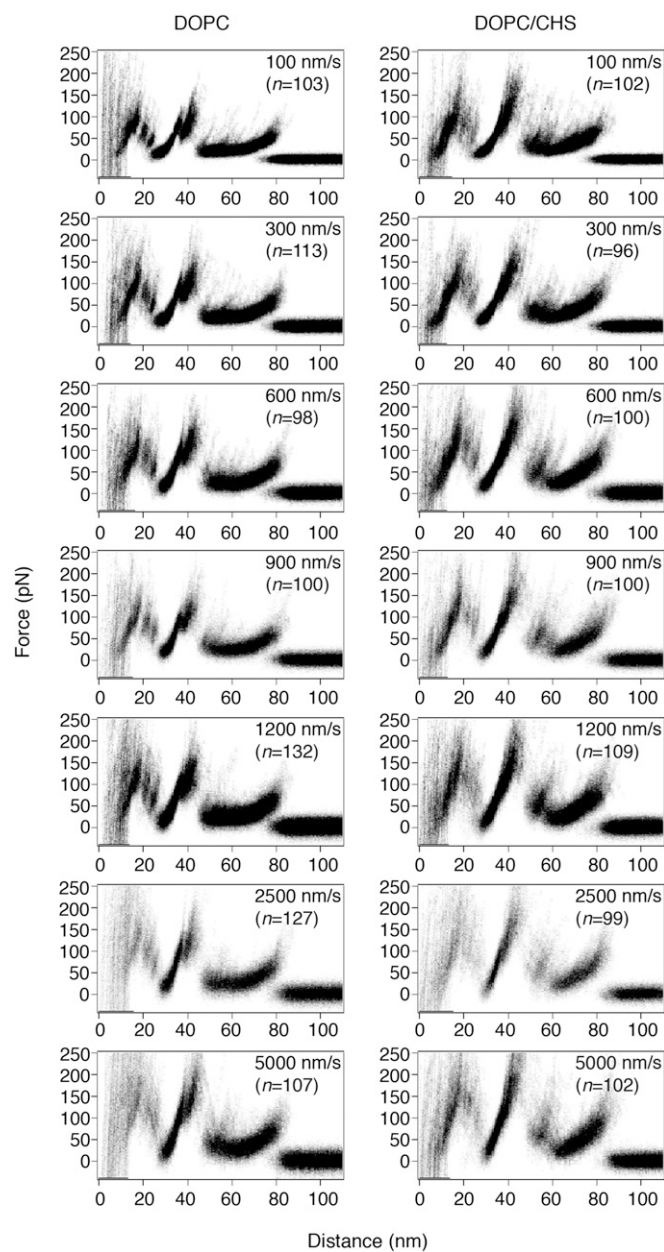


Fig. S6. Superimposed F-D curves recorded on unfolding of β_2 AR reconstituted into DOPC and DOPC/CHS liposomes. Superimposed F-D curves are displayed as density plots. Pulling velocities and numbers (n) of superimposed F-D curves are indicated. F-D curves were aligned at the prominent force peak detected at a contour length of 121 aa. The full gray scale corresponds to 40 counts. Data were recorded in SMFS buffer (300 mM NaCl, 25 mM Tris, 25 mM MgCl₂, pH 7.0).

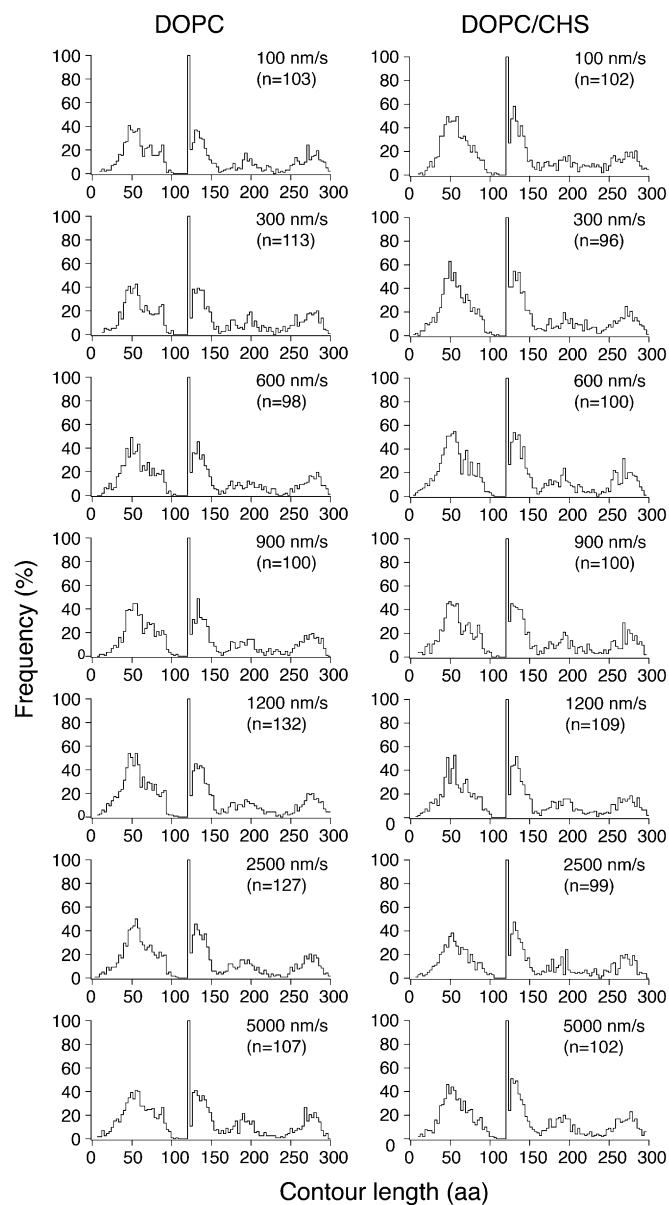


Fig. S7. Frequency of contour lengths at which force peaks were detected on unfolding of β_2 AR reconstituted into DOPC and DOPC/CHS liposomes. Pulling velocities and numbers (n) of F-D curves analyzed are indicated. Bin sizes of histograms are 3 aa. F-D curves were recorded in SMFS buffer (300 mM NaCl, 25 mM Tris, 25 mM $MgCl_2$, pH 7.0) and aligned at the prominent force peak detected at a contour length of 121 aa.

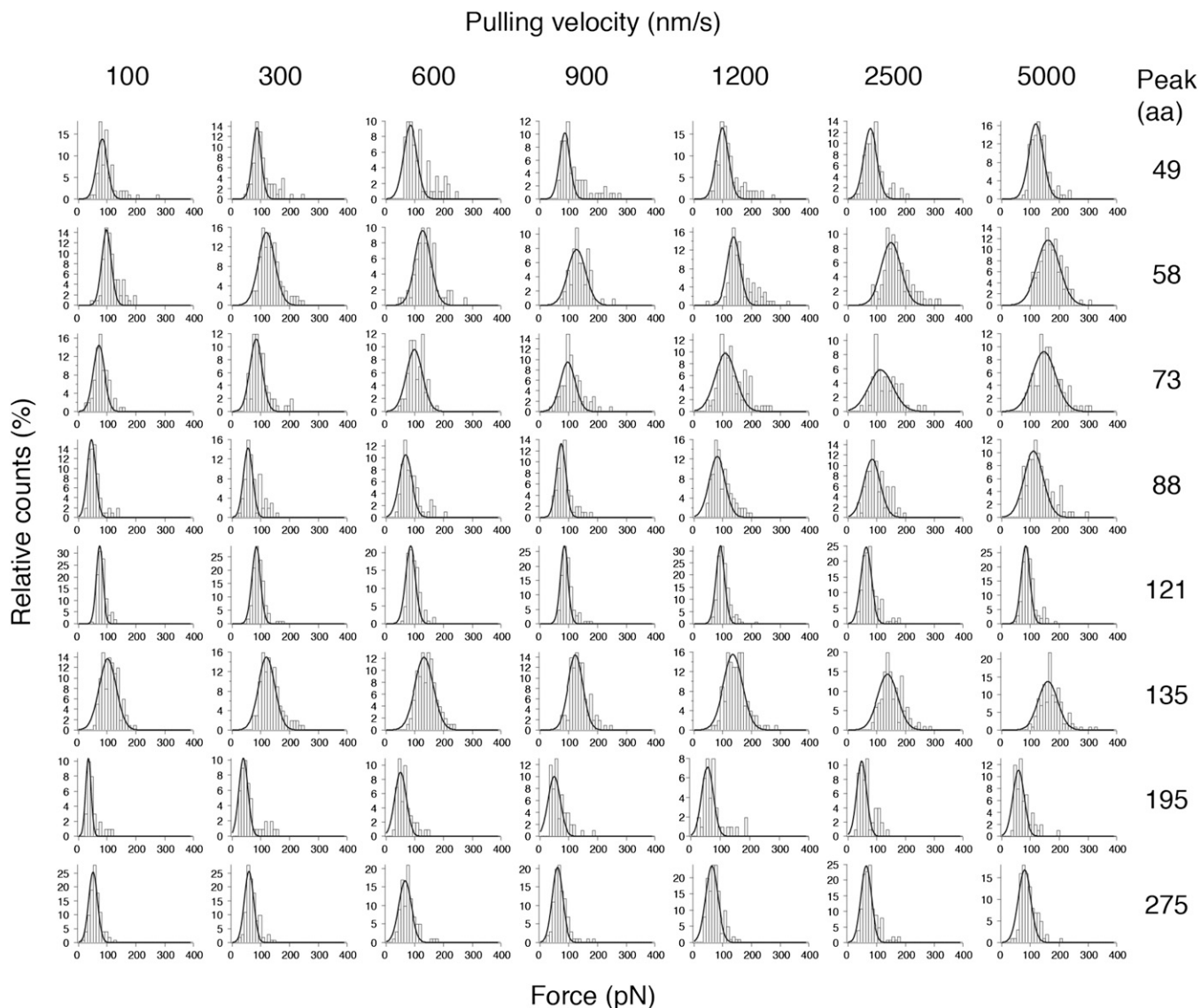


Fig. S8. Unfolding forces of force peaks recorded during unfolding of β_2 AR reconstituted into DOPC liposomes. Histograms show force distributions for every force peak over seven different pulling velocities (100, 300, 600, 900, 1,200, 2,500, and 5,000 nm/s). The bin size of all histograms is 10 pN. Black lines are Gaussian fits of force distributions. Data were recorded in SMFS buffer (300 mM NaCl, 25 mM Tris, 25 mM MgCl₂, pH 7.0).

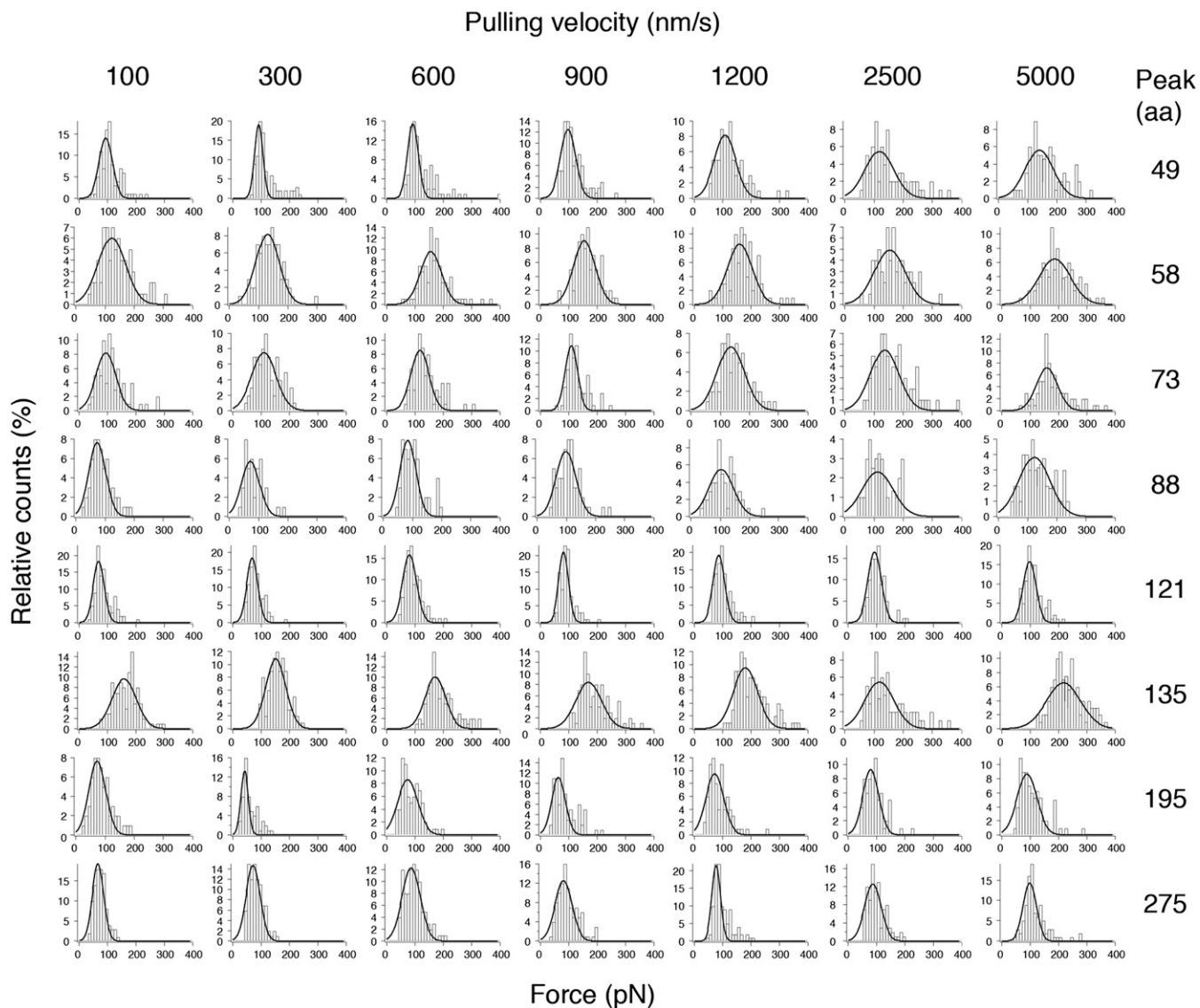


Fig. S9. Unfolding forces of force peaks recorded during unfolding of β_2 AR reconstituted into DOPC/CHS liposomes. Histograms show force distributions for every force peak over seven different pulling velocities (100, 300, 600, 900, 1,200, 2,500, and 5,000 nm/s). The bin size of all histograms is 10 pN. Black lines are Gaussian fits of force distributions. Data were recorded in SMFS buffer (300 mM NaCl, 25 mM Tris, 25 mM MgCl₂, pH 7.0).

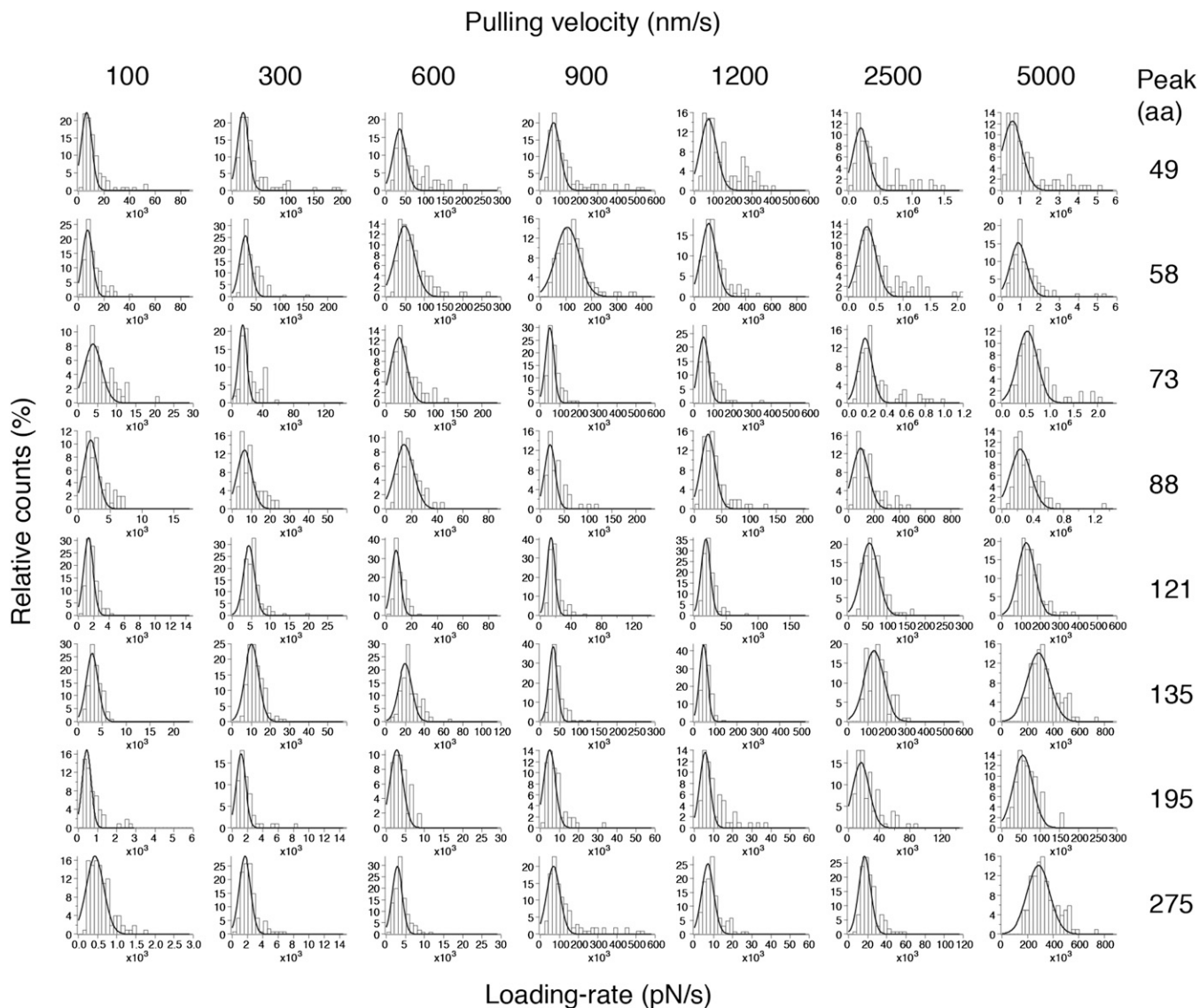


Fig. S10. Loading rates of force peaks recorded during unfolding of β_2 AR reconstituted into DOPC liposomes. Histograms show loading rate distributions for every force peak over seven different pulling velocities (100, 300, 600, 900, 1,200, 2,500, and 5,000 nm/s). Black lines are Gaussian fits of force distributions. Data were recorded in SMFS buffer (300 mM NaCl, 25 mM Tris, 25 mM $MgCl_2$, pH 7.0).

Pulling velocity (nm/s)

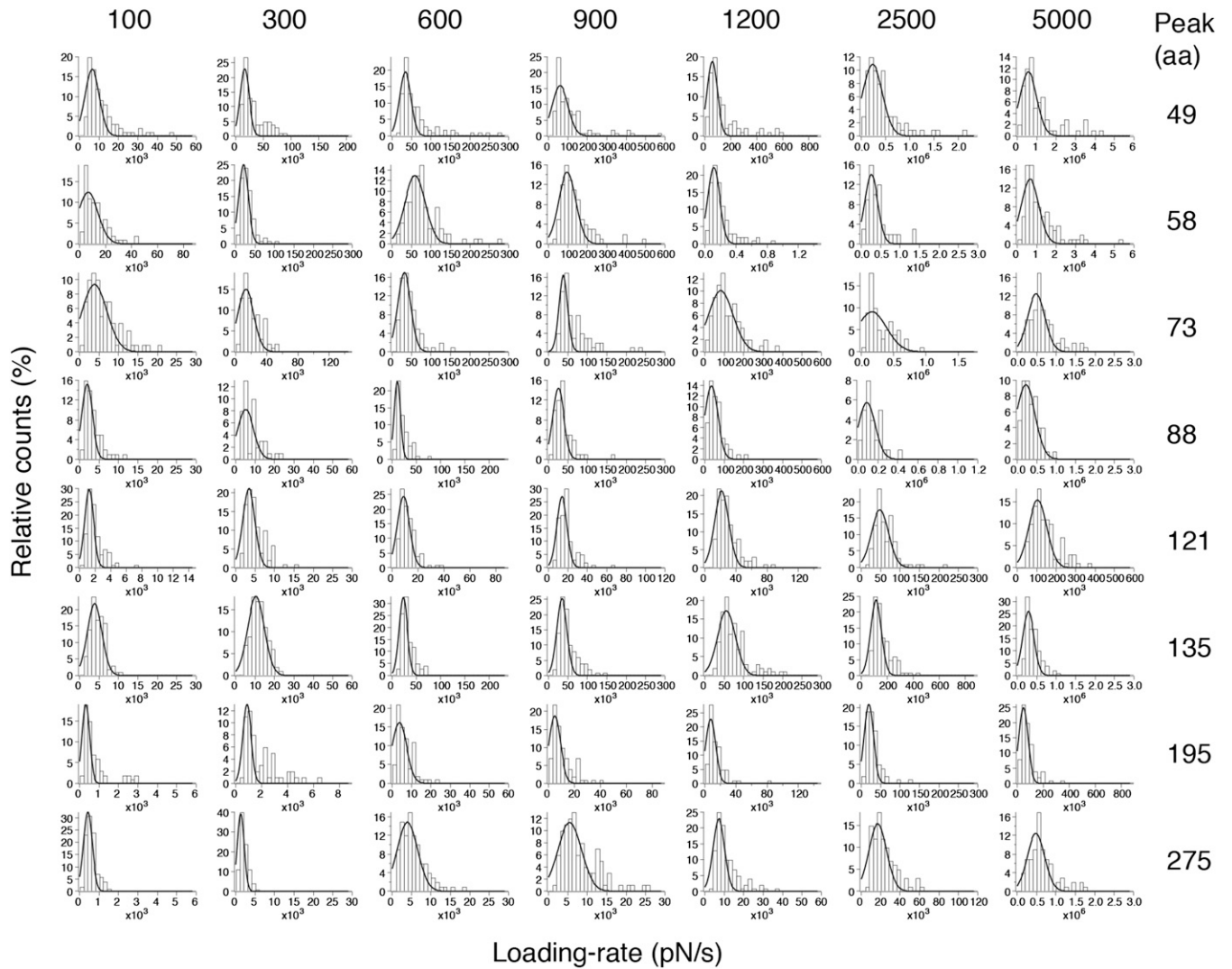


Fig. S11. Loading rates of force peaks recorded during unfolding of β_2 AR reconstituted into DOPC/CHS liposomes. Histograms show loading rate distributions for every force peak over seven different pulling velocities (100, 300, 600, 900, 1,200, 2,500, and 5,000 nm/s). Black lines are Gaussian fits of force distributions. Data were recorded in SMFS buffer (300 mM NaCl, 25 mM Tris, 25 mM $MgCl_2$, pH 7.0).

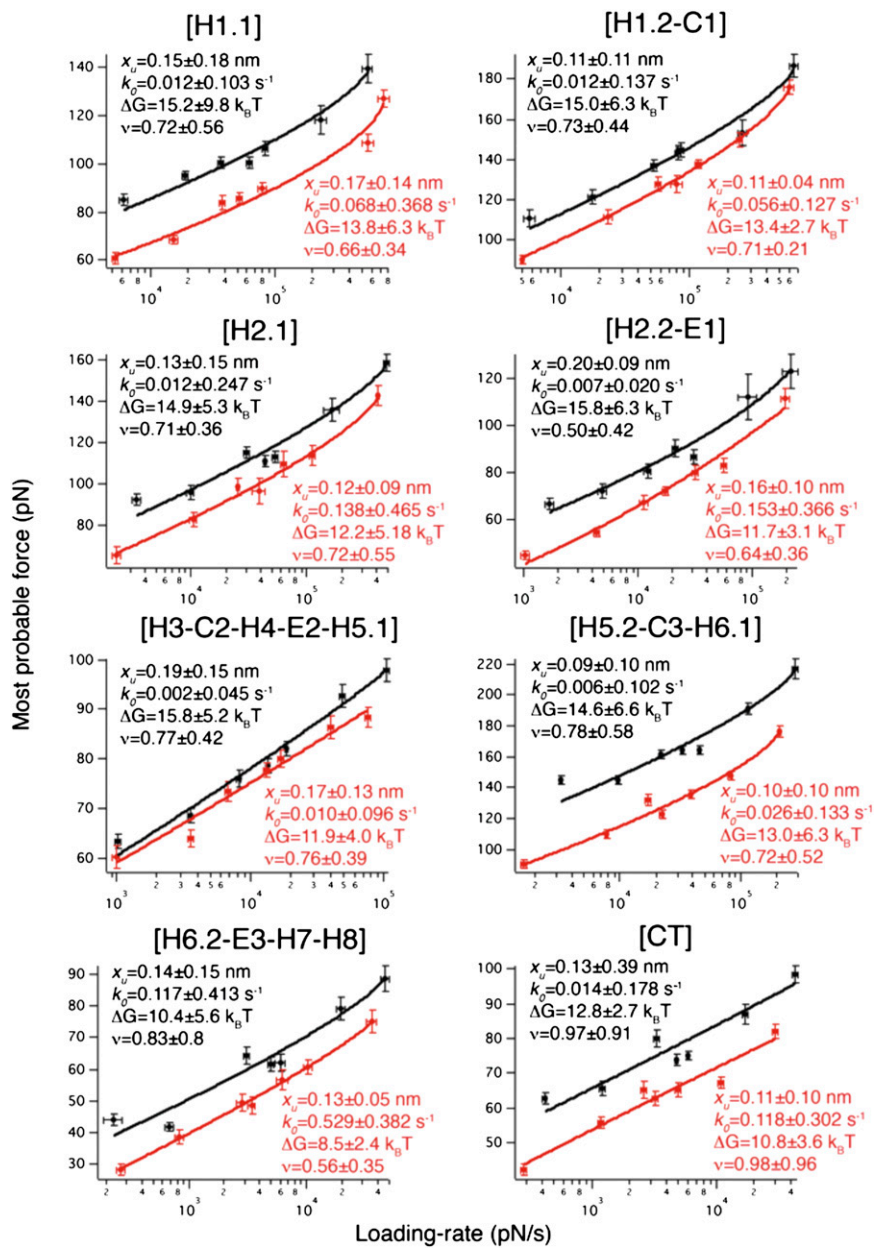


Fig. S12. Alternative dynamic SMFS (DFS) fits using the Dudko–Szabo–Hummer model. DFS plots of each stable structural segment of β_2 AR reconstituted into DOPC (red) and DOPC/CHS (black) liposomes. Shown is the most probable unfolding force against the most probable loading rate. Fitting the DFS plots with the model in the work by Dudko et al. (1) revealed the parameters indicated in each panel. ν is a scaling factor that specifies the profile of the unfolding free-energy barrier (2).

1. Dudko OK, Hummer G, Szabo A (2008) Theory, analysis, and interpretation of single-molecule force spectroscopy experiments. *Proc Natl Acad Sci USA* 105(41):15755–15760.
2. Dudko OK, Hummer G, Szabo A (2006) Intrinsic rates and activation free energies from single-molecule pulling experiments. *Phys Rev Lett* 96(10):108101.

Table S1. Mean contour lengths of force peaks in F-D curves recorded during N-terminal unfolding of unliganded β_2 AR and stable structural segments assigned to the force peaks

Stable structural segment	Contour length \pm SD (aa)	
	DOPC	DOPC/CHS
[H1.1]	49 \pm 4	49 \pm 4
[H1.2-C1]	58 \pm 4	58 \pm 3
[H2.1]	73 \pm 3	73 \pm 3
[H2.2-E1]	88 \pm 4	88 \pm 4
[H3-C2-H4-E2-H5.1]	121 \pm 0*	121 \pm 0*
[H5.2-C3-H6.1]	135 \pm 9	135 \pm 7
[H6.2-E3-H7-H8]	195 \pm 8	195 \pm 7
[CT]	275 \pm 13	275 \pm 11

Contour lengths represent mean peak positions. Errors represent SDs. Number of analyzed F-D curves is $n = 100$ for DOPC and $n = 100$ for DOPC/CHS.

*F-D curves were aligned at the prominent force peak detected at a contour length of 121 aa.

Table S2. Sum of squares F test comparing DFS data recorded from unliganded β_2 AR reconstituted into DOPC/CHS and DOPC liposomes

Liposome	Stable structural segment	Separate SSQ1 (dof1)	SSQ2 (dof2)	Common SSQ (dof)	F ratio	P value
DOPC/CHS	[H1]	154.1 (5)		1,477.8 (12)	21.110	$1.202 \bullet 10^{-4}$
DOPC		128.9 (5)				
DOPC/CHS	[H1.2-C1]	214.0 (5)		860.8 (12)	7.490	$6.464 \bullet 10^{-3}$
DOPC		130.6 (5)				
DOPC/CHS	[H2.1]	253.7 (5)		1,083.1 (12)	9.609	$2.718 \bullet 10^{-3}$
DOPC		117.0 (5)				
DOPC/CHS	[H2.2-E1]	164.5 (5)		1,016.7 (12)	12.028	$1.179 \bullet 10^{-3}$
DOPC		134.0 (5)				
DOPC/CHS	[H3-C2-H4-E2-H5.1]	24.0 (5)		89.6 (12)	0.657	0.597
DOPC		55.2 (5)				
DOPC/CHS	[H5.2-C3-H6.1]	497.7 (5)		4,581.7 (12)	26.153	$4.756 \bullet 10^{-5}$
DOPC		237.6 (5)				
DOPC/CHS	[H6.2-E3-H7-H8]	138.9 (5)		596.4 (12)	14.606	$5.512 \bullet 10^{-4}$
DOPC		13.2 (5)				
DOPC/CHS	[CT]	90.6 (5)		659.3 (12)	18.546	$2.076 \bullet 10^{-4}$
DOPC		49.4 (5)				

For every stable structural segment, we have fitted the DFS plots (Fig. 3) individually and simultaneously using Eq. 1. The difference between the individually or simultaneously fitted values was assessed by the sum of square (SSQ) F tests. Degrees of freedom (dof) are given in parentheses. The F ratio given by $F = ((SSQ1 - SSQ2)/(dof1 - dof2))/(SSQ2/dof2)$ quantifies the relationship between the relative increase in the SSQ and the relative increase in the dof. SSQ1 and SSQ2 refer to the sum of two individual fits compared; dof1 and dof2 denote the dof of two individual fits compared. P values estimate the significance of differences of the same stable structural segment detected of β_2 AR in DOPC/CHS and DOPC liposomes.